

ATP-EMTP evaluation of a new fault location algorithm for three-terminal transmission lines without knowing line parameters

Christos A. Apostolopoulos, George N. Korres
National Technical University of Athens, Greece

ECE Department
Iroon Polytechniou 9
Zografou 15780, Athens, Greece
apostolo@power.ece.ntua.gr, gkorres@softlab.ece.ntua.gr

Abstract – *This paper presents a new algorithm for locating faults in three-terminal transmission lines without requiring line parameters. The voltages and currents from all terminals are taken as inputs and no synchronization is needed. The proposed algorithm is based on distributed parameter line model which fully considers the effects of shunt capacitance of the line. Using prefault data, the synchronization angles between measurements at the reference terminal and the other two terminals are determined. Furthermore, positive sequence line parameters are estimated as byproduct at this stage. Using fault data and the parameter estimates obtained at the previous stage, the faulted line section is identified initially. Afterwards, the location of the fault in the faulted line section is determined. Zero sequence line parameters might also be estimated at this stage if the fault has involved earth. The proposed algorithm has been tested extensively with reliable fault data obtained from ATP-EMTP simulations. Some representative results are reported and discussed.*

Keywords: *ATP-EMTP, fault location, three-terminal transmission line, distributed parameter line model, transmission line parameter estimation.*

1 Introduction

Fast and accurate fault location is a key task for accelerating system restoration, reducing outage times and, hence, improving system reliability. While numerous fault location methods have been proposed in the literature, most of them require that the electrical parameters of the line are well known. However, this does not always stand true. In fact, the line parameters including series resistance and inductance and shunt capacitance of the line are generally not known with a great precision. Especially in the zero sequence, several factors influence accuracy. While these imprecise parameters may be sufficient for protection purposes, a higher accuracy is an important requirement for the fault location.

Recent methods that obviate the need for knowing line parameters have been described in [1]-[3]. These methods utilize unsynchronized voltage and currents fault recordings obtained from both terminals of a transmission line in order to determine the fault location without the latter being affected by line parameter errors. The results achieved are highly accurate. Furthermore, these methods can provide fairly accurate estimates for the transmission line parameters by taking advantage of both the prefault and fault data in the fault recordings. The

derived line parameters can also be useful inputs to all sorts of power system analysis programs.

The previously discussed methods for fault location are limited only to two-terminal lines. This paper extends their applicability to three-terminal lines also. Three-terminal lines often offer considerable advantages and benefits over two-terminal lines for EHV purposes, which in many cases are not readily solved using conventional methods. However, from the protection viewpoint, three-terminal lines impose critical restrictions and pose great difficulties in accurately locating faults in their sections.

In this paper, a new algorithm for locating faults in three-terminal transmission lines without knowing line parameters is presented. The algorithm utilizes the fundamental frequency phasors from the three ends of the line based on ideally transposed distributed parameter line model, which fully considers the shunt capacitance and distributed parameter effects. The developed algorithm is independent of fault resistance and source impedance, and does not require data synchronization between measurements at the three ends of the line. Furthermore, the positive and zero sequence line parameters (**only** for single-line-to-ground faults) can be obtained as a byproduct of the method.

Section 2 presents the proposed algorithm. The evaluation studies using comprehensive ATP-EMTP simulations are reported in Section 3. A conclusion is drawn in section 4.

2 Fault location and line parameter estimation for three-terminal lines

In this paper, we consider a transposed line between three terminals S, R and T. The following discussion assumes that unsynchronized voltage and current fault recordings are available at each line terminal for a fault occurring on one of the line sections. Fig. 1 represents the positive sequence network of the system under study before the fault occurrence. Figs. 2 and 3 depict the positive, negative and zero sequence networks of the system during a fault on the line section SM. M and F indicate the tap and fault point respectively.

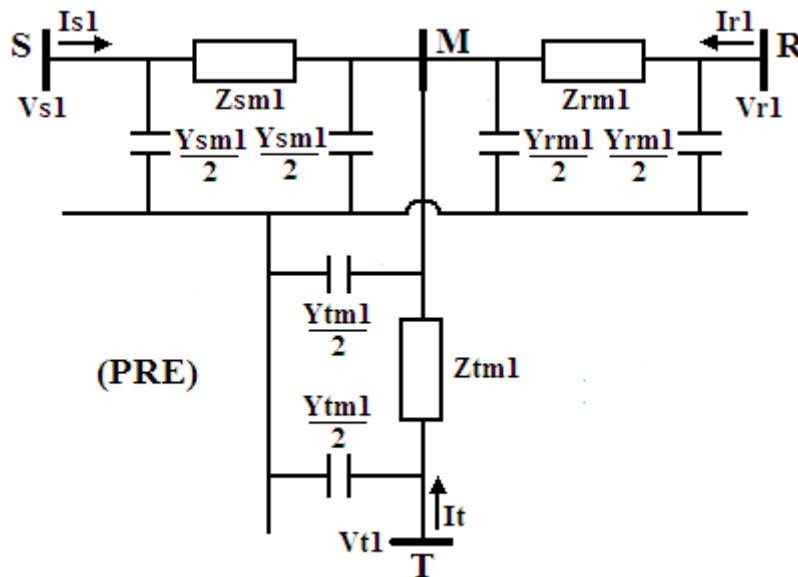


Fig. 1. Positive sequence network of the system preceding the fault

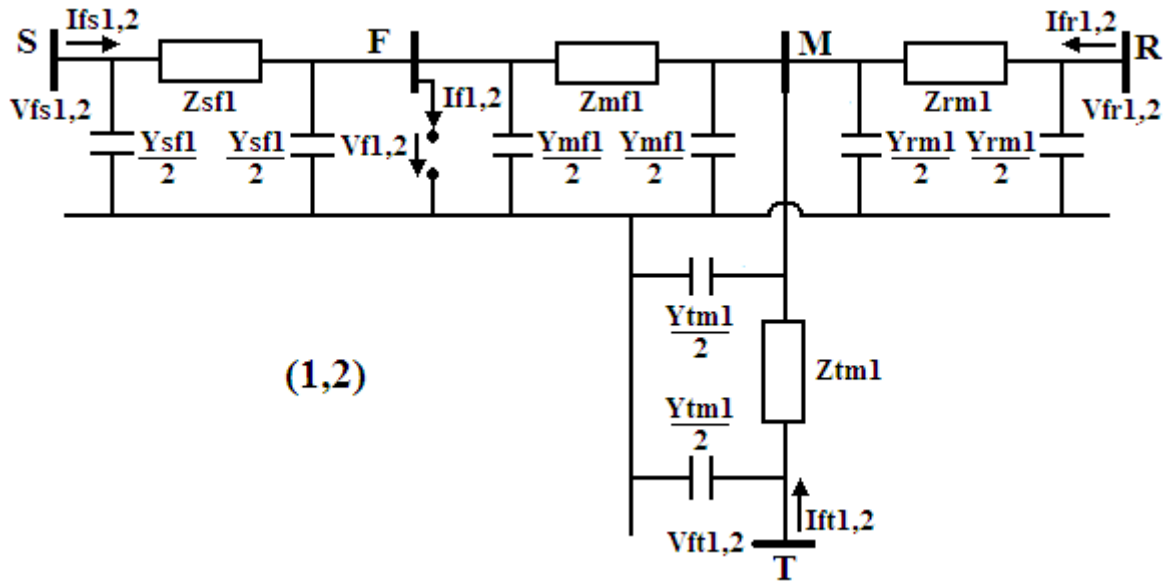


Fig. 2. Positive and negative sequence networks of the system during the fault

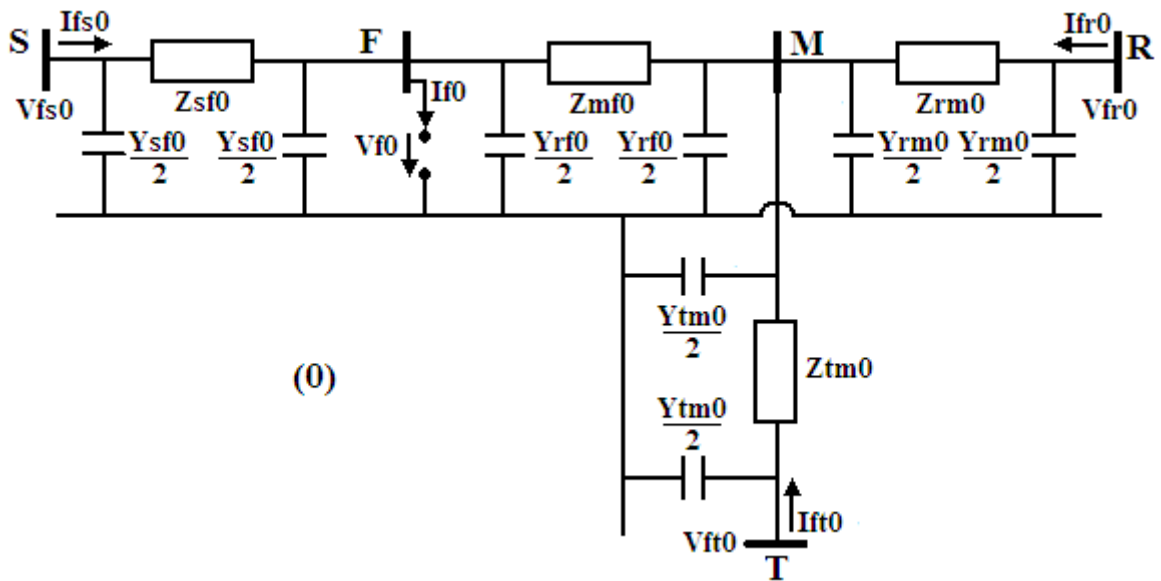


Fig. 3. Zero sequence network of the system during the fault

Considering the above figures the following notations are employed.

$Z_{sm1}, Z_{rm1}, Z_{tm1}, Z_{sf1}, Z_{mf1}$: equivalent positive sequence series impedances of line sections SM, RM, TM, SF and MF;

$Z_{sm0}, Z_{rm0}, Z_{tm0}, Z_{sf0}, Z_{mf0}$: equivalent zero sequence series impedances of line sections SM, RM, TM, SF and MF;

$Y_{sm1}, Y_{rm1}, Y_{tm1}, Y_{sf1}, Y_{mf1}$: equivalent positive sequence shunt admittances of line sections SM, RM, TM, SF and MF;

$Z_{sm0}, Z_{rm0}, Z_{tm0}, Z_{sf0}, Z_{mf0}$: equivalent zero sequence shunt admittances of line sections SM, RM, TM, SF and MF;

V_{s1}, V_{r1}, V_{t1} : pre-fault positive sequence voltages at S, R and T;
 I_{s1}, I_{r1}, I_{t1} : pre-fault positive sequence currents at S, R and T;
 $V_{fs1}, V_{fr1}, V_{ft1}, V_{f1}$: positive sequence voltages during the fault at S, R, T and F;
 $V_{fs2}, V_{fr2}, V_{ft2}, V_{f2}$: negative sequence voltages during the fault at S, R, T and F;
 $V_{fs0}, V_{fr0}, V_{ft0}, V_{f0}$: zero sequence voltages during the fault at S, R, T and F;
 $I_{fs1}, I_{fr1}, I_{ft1}, I_{f1}$: positive sequence currents during the fault at S, R, T and F;
 $I_{fs2}, I_{fr2}, I_{ft2}, I_{f2}$: negative sequence currents during the fault at S, R, T and F;
 $I_{fs0}, I_{fr0}, I_{ft0}, I_{f0}$: zero sequence currents during the fault at S, R, T and F;

The equivalent line parameters are computed based on distributed parameter line model as follows [4]:

$$Z_{smi} = Z_{ci} \sinh(\gamma_i l_1) \quad (1)$$

$$Z_{rmi} = Z_{ci} \sinh(\gamma_i l_2) \quad (2)$$

$$Z_{tmi} = Z_{ci} \sinh(\gamma_i l_3) \quad (3)$$

$$Z_{sfi} = Z_{ci} \sinh(\gamma_i l) \quad (4)$$

$$Z_{mfi} = Z_{ci} \sinh(\gamma_i (l_1 - l)) \quad (5)$$

$$Y_{smi} = (2/Z_{ci}) \tanh(\gamma_i l_1/2) \quad (6)$$

$$Y_{rmi} = (2/Z_{ci}) \tanh(\gamma_i l_2/2) \quad (7)$$

$$Y_{tmi} = (2/Z_{ci}) \tanh(\gamma_i l_3/2) \quad (8)$$

$$Y_{sfi} = (2/Z_{ci}) \tanh(\gamma_i l/2) \quad (9)$$

$$Y_{mfi} = (2/Z_{ci}) \tanh(\gamma_i (l_1 - l)/2) \quad (10)$$

$$Z_{ci} = \sqrt{z_i/y_i} \quad (11)$$

$$\gamma_i = \sqrt{z_i y_i} \quad (12)$$

where: $i=0,1$; l_1 , l_2 and l_3 are the lengths of the line sections SM, RM and TM in mile or km, respectively; l is the distance to fault point F from S (or R and T respectively) in miles or km; Z_{ci} and γ_i are the characteristic impedances and propagation constants of the line, respectively; $z_i = r_i + jx_i$ and $y_i = jb_i$ are the series impedances and shunt admittances of the line per mile or km, respectively, with r_i , x_i and b_i being the series resistances, reactances, and shunt susceptances per mile or km.

The complete algorithm for fault location and parameter line estimation is very complex and comprises the following tasks:

- ✓ phasor estimation, fault type detection, fault recording segmentation and data alignment
- ✓ positive sequence parameters estimation and synchronization error determination using pre-fault data
- ✓ faulted section selection using fault data
- ✓ fault location and zero sequence parameters estimation (if possible) using fault data

The above mentioned tasks and their implementation issues are discussed in the following paragraphs.

2.1 Phasor estimation, fault type detection, fault recording segmentation and data alignment

Since the proposed algorithm uses the fundamental voltage and current phasors from all line ends, the voltage and current waveforms captured by digital fault recorders (DFRs) at each terminal must be converted into fundamental frequency phasors. This is done using a two-stage approach. In the first stage, the voltage and current signals are filtered by a low-pass filter to remove possible noise and higher harmonics. In the second stage, the fundamental phasors are calculated using the conventional full-cycle DFT algorithm with synchronous sampling [5]. When fault recordings do not originate from DFRs but are produced by digital relays with precalculated signal phasors, the algorithm is still capable of manipulating them via the Comtrade data format [6].

After computing the voltage and current phasors at each terminal, the next step is to determine the fault type and inception time. Fault type selection is very important, since different equations corresponding to boundary fault conditions are utilized for each fault type. Therefore, the highly secure algorithm of [7] has been adopted for fault type classification.

Through the fault type selection process, it is also possible to determine the time instant of the fault initialization. Using this information, we can segment the recorded signals into pre-fault and fault parts.

The final task is to align the fault recording data for further processing. The fault recordings are usually obtained from non synchronized DFRs or digital relays located at each line terminal. To synchronize them, we detect the fault instant in all analog signals and we choose the recording with the minimum fault inception time as the reference one. Then, we synchronize the remaining recordings with the reference recording, by equating their fault inception times with the reference fault inception time; i.e., we left-shift these recordings, until fault inception times become equal to the reference one.

2.2 Positive sequence parameter estimation and synchronization error determination using pre-fault data

The proposed algorithm utilizes the voltage and current phasors from the three terminals before the fault, in order to estimate positive sequence line parameters as well as to refine the synchronization of phasors. However, there is still need to refine synchronization of phasors because errors with more than one sampling interval may arise after the segmentation phase. To solve this problem, we use the following procedure. From Fig. 1, the following equations for voltage and currents at the tap point M are obtained:

$$V_{m1,s} = V_{s1}(1 + (Y_{sm1}/2)Z_{sm1}) - I_{s1}Z_{sm1} \quad (13)$$

$$V_{m1,r} = (V_{r1}(1 + (Y_{rm1}/2)Z_{rm1}) - I_{r1}Z_{rm1})e^{j\delta} \quad (14)$$

$$V_{m1,t} = (V_{t1}(1 + (Y_{tm1}/2)Z_{tm1}) - I_{t1}Z_{tm1})e^{j\phi} \quad (15)$$

$$I_{sm1} = (I_{s1} - V_{s1}(Y_{sm1}/2)) - (V_{s1} - (I_{s1} - V_{s1}(Y_{sm1}/2))Z_{sm1})(Y_{sm1}/2) \quad (16)$$

$$I_{rm1} = ((I_{r1} - V_{r1}(Y_{rm1}/2)) - (V_{r1} - (I_{r1} - V_{r1}(Y_{rm1}/2))Z_{rm1})(Y_{rm1}/2))e^{j\delta} \quad (17)$$

$$I_{tm1} = ((I_{t1} - V_{t1}(Y_{tm1}/2)) - (V_{t1} - (I_{t1} - V_{t1}(Y_{tm1}/2))Z_{tm1})(Y_{tm1}/2))e^{j\varphi} \quad (18)$$

where δ and φ are the synchronization angles between measurements at S and R and S and T respectively, representing any possible synchronization error.

Based on Fig. 1 and equations (13)-(18), we can derive the following equations:

$$f_1(X) = V_{m1,s} - V_{m1,r} = V_{s1}(1 + (Y_{sm1}/2)Z_{sm1}) - I_{s1}Z_{sm1} - (V_{r1}(1 + (Y_{rm1}/2)Z_{rm1}) - I_{r1}Z_{rm1})e^{j\delta} = 0 \quad (19)$$

$$f_2(X) = V_{m1,s} - V_{m1,t} = V_{s1}(1 + (Y_{sm1}/2)Z_{sm1}) - I_{s1}Z_{sm1} - (V_{t1}(1 + (Y_{tm1}/2)Z_{tm1}) - I_{t1}Z_{tm1})e^{j\phi} = 0 \quad (20)$$

$$\begin{aligned} f_3(X) &= I_{sm1} + I_{rm1} + I_{tm1} = \\ &= (I_{s1} - V_{s1}(Y_{sm1}/2)) - (V_{s1} - (I_{s1} - V_{s1}(Y_{sm1}/2))Z_{sm1})(Y_{sm1}/2) \\ &\quad + ((I_{r1} - V_{r1}(Y_{rm1}/2)) - (V_{r1} - (I_{r1} - V_{r1}(Y_{rm1}/2))Z_{rm1})(Y_{rm1}/2))e^{j\delta} \\ &\quad + ((I_{t1} - V_{t1}(Y_{tm1}/2)) - (V_{t1} - (I_{t1} - V_{t1}(Y_{tm1}/2))Z_{tm1})(Y_{tm1}/2))e^{j\phi} \\ &= 0 \end{aligned} \quad (21)$$

where X is defined as the unknown variable vector and T symbolizes the vector transpose operator. Let us define $F(X)$ as a function vector composed of the following elements:

$$F_{2i-1}(X) = \text{Re}(f_i(X)), \quad i = 1, \dots, 3 \quad (22)$$

$$F_{2i}(X) = \text{Im}(f_i(X)), \quad i = 1, \dots, 3 \quad (23)$$

Then the five unknown variables can be obtained using the well-known least squares approach which computes the correction ΔX_k at each iteration:

$$\Delta X_k = -J^{-1}(X_k)F(X_k) \quad (24)$$

where, $k = 0, 1, 2, \dots$ is the iteration count, $\Delta X_k = X_{k+1} - X_k$ is the variable update vector, and $J(X_k) = \partial F(X_k)/\partial X$ is the Jacobian matrix at k th iteration. The iterative process can be terminated when the variable update is less than a specified tolerance.

The derivative of $F_1(X)$ with respect to the unknown variable r_1 can be determined as follows:

$$\begin{aligned} \frac{\partial f_1(X)}{\partial r_1} &= \left(\frac{l_1 \sinh(\gamma_1 l_1)}{2 \cosh^2(\gamma_1 l_1/2)} \frac{\partial \gamma_1}{\partial r_1} + l_1 \tanh(\gamma_1 l_1/2) \cosh(\gamma_1 l_1) \frac{\partial \gamma_1}{\partial r_1} \right) V_{s1} \\ &\quad - \left(\sinh(\gamma_1 l_1) \frac{\partial Z_{c1}}{\partial r_1} + l_1 Z_{c1} \cosh(\gamma_1 l_1) \frac{\partial \gamma_1}{\partial r_1} \right) I_{s1} \\ &\quad - \left(\frac{l_2 \sinh(\gamma_1 l_2)}{2 \cosh^2(\gamma_1 l_2/2)} \frac{\partial \gamma_1}{\partial r_1} + l_2 \tanh(\gamma_1 l_2/2) \cosh(\gamma_1 l_2) \frac{\partial \gamma_1}{\partial r_1} \right) V_{r1} e^{j\delta} \\ &\quad + \left(\sinh(\gamma_1 l_2) \frac{\partial Z_{c1}}{\partial r_1} + l_2 Z_{c1} \cosh(\gamma_1 l_2) \frac{\partial \gamma_1}{\partial r_1} \right) I_{r1} e^{j\delta} \end{aligned} \quad (25)$$

and

$$\frac{\partial \gamma_1}{\partial r_1} = \frac{\sqrt{jb_1}}{2\sqrt{r_1 + jx_1}} \quad (26)$$

$$\frac{\partial Z_{c1}}{\partial r_1} = \frac{1}{2\sqrt{r_1 + jx_1}\sqrt{jb_1}} \quad (27)$$

From (22) and (25)-(28) we obtain:

$$\frac{\partial F_1(X)}{\partial r_1} = \text{Re} \left(\frac{\partial f_1(X)}{\partial r_1} \right). \quad (28)$$

The partial derivatives of the other elements of $F(X)$ with respect to the unknown variables can be obtained similarly.

2.3 Faulted line section selection using fault data

After determining the positive sequence line parameters and the synchronization angles, the next step of the algorithm is to select the faulted section in the three-terminal transmission line.

As shown in Fig. 2 and Fig. 3, the fault lies in a section of length l with respect to terminal S. Using the positive sequence voltages and currents, the lengths of each section with respect to the tap point and the line impedances of each section, the tap point voltages $V_{fm1,s}$, $V_{fm1,r}$ and $V_{fm1,t}$ can be calculated from the following equations:

$$V_{fm1,s} = V_{fs1}(1 + (Y_{sm1}/2)Z_{sm1}) - I_{fs1}Z_{sm1} \quad (29)$$

$$V_{fm1,r} = (V_{fr1}(1 + (Y_{rm1}/2)Z_{rm1}) - I_{fr1}Z_{rm1})e^{j\delta} \quad (30)$$

$$V_{fm1,t} = (V_{ft1}(1 + (Y_{tm1}/2)Z_{tm1}) - I_{ft1}Z_{tm1})e^{j\phi} \quad (31)$$

By using the calculated tap point voltages, we obtain the following differentials [8]:

$$\Delta V_{m,sr} = |V_{fm1,s} - V_{fm1,r}| \quad (32)$$

$$\Delta V_{m,rt} = |V_{fm1,r} - V_{fm1,t}| \quad (33)$$

$$\Delta V_{m,ts} = |V_{fm1,t} - V_{fm1,s}| \quad (34)$$

Since we have assumed that the fault has occurred in section SM, it is clear that $\Delta V_{m,sr} > 0$, $\Delta V_{m,ts} > 0$ and $\Delta V_{m,rt} \approx 0$. This can lead us to the criterion for selecting the faulted section in respect of a three-terminal transmission line: $\min(\Delta V_{m,sr}, \Delta V_{m,rt}, \Delta V_{m,ts})$. The minimum differential indicates the ‘‘sound’’ line sections.

2.4 Fault location and zero sequence parameters estimation (if possible) using fault data

The faulted section can be determined using the criterion described above. Afterwards, the fault location can be estimated by converting the three-terminal transmission line into a two-terminal transmission line, which includes the fault point, and using the boundary fault conditions that exist for each fault type. From Fig. 2 and 3, we can derive the following equations:

$$V_{f1,s} = V_{fs1}(1 + (Y_{sf1}/2)Z_{sf1}) - I_{fs1}Z_{sf1} \quad (35)$$

$$V_{f2,s} = V_{fs2}(1 + (Y_{sf1}/2)Z_{sf1}) - I_{fs2}Z_{sf1} \quad (36)$$

$$V_{f0,s} = V_{fs0}(1 + (Y_{sf0}/2)Z_{sf0}) - I_{fs0}Z_{sf0} \quad (37)$$

$$I_{f1,s} = (I_{fs1} - V_{fs1}(Y_{sf1}/2)) - (V_{fs1} - (I_{fs1} - V_{fs1}(Y_{sf1}/2))Z_{sf1})(Y_{sf1}/2) \quad (38)$$

$$I_{f2,s} = (I_{fs2} - V_{fs2}(Y_{sf1}/2)) - (V_{fs2} - (I_{fs2} - V_{fs2}(Y_{sf1}/2))Z_{sf1})(Y_{sf1}/2) \quad (39)$$

$$I_{f0,s} = (I_{fs0} - V_{fs0}(Y_{sf0}/2)) - (V_{fs0} - (I_{fs0} - V_{fs0}(Y_{sf0}/2))Z_{sf0})(Y_{sf0}/2) \quad (40)$$

$$I_{fm1,r} = ((I_{fr1} - V_{fr1}(Y_{rm1}/2)) - (V_{fr1} - (I_{fr1} - V_{fr1}(Y_{rm1}/2))Z_{rm1})(Y_{rm1}/2))e^{j\delta} \quad (41)$$

$$I_{fm2,r} = ((I_{fr2} - V_{fr2}(Y_{rm1}/2)) - (V_{fr2} - (I_{fr2} - V_{fr2}(Y_{rm1}/2))Z_{rm1})(Y_{rm1}/2))e^{j\delta} \quad (42)$$

$$I_{fm0,r} = ((I_{fr0} - V_{fr0}(Y_{rm0}/2)) - (V_{fr0} - (I_{fr0} - V_{fr0}(Y_{rm0}/2))Z_{rm0})(Y_{rm0}/2))e^{j\delta} \quad (43)$$

$$I_{fm1,t} = ((I_{ft1} - V_{ft1}(Y_{tm1}/2)) - (V_{ft1} - (I_{ft1} - V_{ft1}(Y_{tm1}/2))Z_{tm1})(Y_{tm1}/2))e^{j\phi} \quad (44)$$

$$I_{fm2,t} = ((I_{ft2} - V_{ft2}(Y_{tm1}/2)) - (V_{ft2} - (I_{ft2} - V_{ft2}(Y_{tm1}/2))Z_{tm1})(Y_{tm1}/2))e^{j\phi} \quad (45)$$

$$I_{fm0,t} = ((I_{ft0} - V_{ft0}(Y_{tm0}/2)) - (V_{ft0} - (I_{ft0} - V_{ft0}(Y_{tm0}/2))Z_{tm0})(Y_{tm0}/2))e^{j\phi} \quad (46)$$

By combining (30) and (41)-(46), we obtain the positive, negative and zero sequence voltages and currents at the fault point F as seen from the tap point M:

$$V_{f1,m} = V_{fm1,r}(1 + (Y_{mf1}/2)Z_{mf1}) - (I_{fm1,r} + I_{fm1,t})Z_{mf1} \quad (47)$$

$$V_{f2,m} = V_{fm2,r}(1 + (Y_{mf1}/2)Z_{mf1}) - (I_{fm2,r} + I_{fm2,t})Z_{mf1} \quad (48)$$

$$V_{f0,m} = V_{fm0,r}(1 + (Y_{mf0}/2)Z_{mf0}) - (I_{fm0,r} + I_{fm0,t})Z_{mf0} \quad (49)$$

$$I_{f1,m} = (I_{fm1,r} + I_{fm1,t}) - V_{fm1,r}(Y_{mf1}/2) - (V_{fm1,r} - ((I_{fm1,r} + I_{fm1,t}) - V_{fm1,r}(Y_{mf1}/2))Z_{mf1})(Y_{mf1}/2) \quad (50)$$

$$I_{f2,m} = (I_{fm2,r} + I_{fm2,t}) - V_{fm2,r}(Y_{mf1}/2) - (V_{fm2,r} - ((I_{fm2,r} + I_{fm2,t}) - V_{fm2,r}(Y_{mf1}/2))Z_{mf1})(Y_{mf1}/2) \quad (51)$$

$$I_{f0,m} = (I_{fm0,r} + I_{fm0,t}) - V_{fm0,r}(Y_{mf0}/2) - (V_{fm0,r} - ((I_{fm0,r} + I_{fm0,t}) - V_{fm0,r}(Y_{mf0}/2))Z_{mf0})(Y_{mf0}/2) \quad (52)$$

Considering the boundary fault conditions at the fault point, we have for each fault type:

A. For three-phase (LLL) fault

The following condition is met:

$$f_4(l) = V_{f1,s} - V_{f1,m} = 0 \quad (53)$$

Based on (53) we define the function:

$$F_4(l) = abs(f_4(l)). \quad (54)$$

B. For line-to-line (LL) fault

Let us consider the phase B to C fault. Equation (53) and the following equations are met:

$$f_5(l) = V_{f2,s} - V_{f2,m} = 0 \quad (55)$$

$$f_6(l) = (I_{f1,s} + I_{f1,m}) + (I_{f2,s} + I_{f2,m}) = 0 \quad (56)$$

Combining (53), (55) and (56), we can define the function:

$$F_5(l) = \text{abs}(f_4(l)) + \text{abs}(f_5(l)) + \text{abs}(f_6(l)). \quad (57)$$

The same function can be applied for all the line-to-line faults.

C. For line-to-line-to-ground (LLG) fault

Let us assume the phase B to C to ground fault as an instance. Except for (53) and (55), the following equation applies:

$$f_7(l) = V_{f1,s} - V_{f2,s} = 0 \quad (58)$$

Combining (53), (55) and (58), we can define the function:

$$F_6(l) = \text{abs}(f_4(l)) + \text{abs}(f_5(l)) + \text{abs}(f_7(l)). \quad (59)$$

The same function can be used for all the line-to-line-ground faults.

D. For single-line-to-ground (LG) fault

In this case, we can also estimate the zero-sequence line parameters. Let us consider the phase A to ground fault. Then, the following equations apply:

$$f_8(X') = V_{f2,s} - V_{f2,m} = 0 \quad (60)$$

$$f_9(X') = V_{f0,s} - V_{f0,m} = 0 \quad (61)$$

$$f_{10}(X') = (I_{f2,s} + I_{f2,m}) - (I_{f0,s} + I_{f0,m}) = 0 \quad (62)$$

where X' is the unknown variable vector: $X' = [r_0, x_0, b_0, l]^T$. We define by $F(X')$ a vector function having the following elements:

$$F_{2i-1}(X) = \text{Re}(f_i(X)), \quad i = 4, \dots, 6 \quad (63)$$

$$F_{2i}(X) = \text{Im}(f_i(X)), \quad i = 4, \dots, 6 \quad (64)$$

Similar functions can be used for single-line-to-ground faults involving phases B or C. For fault types A, B and C, the unknown variables can be found using the Newton-Raphson method, while for single-line-to-ground faults they can be found using the well-established least squares algorithm, as described in §2.2.

3 ATP-EMTP evaluation studies

This section presents evaluation studies based on ATP-EMTP simulation data. A 400-kV power network containing a three-terminal transmission line is adopted here. The parameters of the network are gathered at Table 1. The line is modeled based on distributed parameter line model. Several fault types with different fault locations and fault resistances have been simulated to generate voltage and current waveforms. These waveforms are filtered with a 4th order Butterworth low-pass anti-aliasing filter to remove noise. Then the full-cycle DFT with a sampling frequency of 1000 Hz is applied to extract the fundamental voltage and current phasors to evaluate the performance of the proposed fault location and line parameters estimation algorithm for three-terminal lines.

Due to the fact that the data obtained from ATP-EMTP are already time-aligned, the part of the algorithm that is assigned with this task is skipped. All the other tasks are executed. To simulate synchronization errors, we have rotated the phasors at terminals R and T by 18° and 36° respectively in all cases studied.

The proposed algorithms presented have been implemented in Matlab. In order to demonstrate the whose process of the algorithm an analytical example is given for an A-G fault with fault resistance $R_f = 10$ Ohm at 40% of line section SM. Figs. 4, 5 and 6 display the positive, negative and zero sequence voltage and current phasors at each terminal of the line with respect to their magnitude.

The fault type selection algorithm recognizes the fault as a single-line-to-ground fault involving phase A and identifies the pre-fault and fault segments of the fault recordings. Using the pre-fault data and applying the least-squares method, the unknown X can be estimated. To estimate X , the iteration process is terminated when the update is less than $1E-6$.

The initial values for X adopted here are: $X_0 = [0.1, 1.0, 3.1416E-5, 0, 0]$. To speed-up the convergence, the line parameters $r1$, $x1$ and $b1$ are constrained as positive values while the synchronization angles are bounded between $-\pi$ and π . The results obtained after 6 iterations are presented in Table 2. The parameters accuracy is measured by the percentage error calculated by:

$$\frac{|\text{Actual parameter value} - \text{Estimated parameter value}|}{\text{Actual parameter value}} \times 100 \quad (65)$$

It is demonstrated in Table 2 that highly precise results have been obtained for the positive sequence line parameters. After estimating the positive sequence line parameters and the synchronization angles, the algorithm determines the faulted section of the three-terminal line using the criterion presented in §2.3. Fig. 7 shows the voltage differentials calculated at the tap point M using (32)-(34). From Fig. 7, it is evident that the fault lies on section SM. Applying the least-squares method presented in §2.4 with initial values $X_0' = [0.5, 1.5, 1.5708E-5, 75]$, it yields after 7 iterations the results depicted in Table 2 for fault location and zero sequence line parameters. It is obvious that quite accurate results have been achieved.

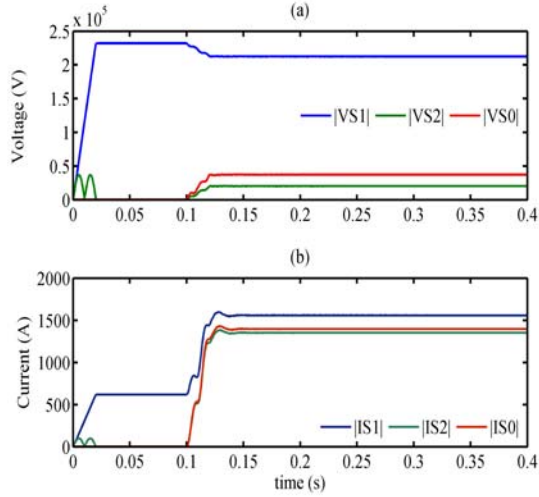


Fig. 4. Sequence voltage and current phasors magnitude at S

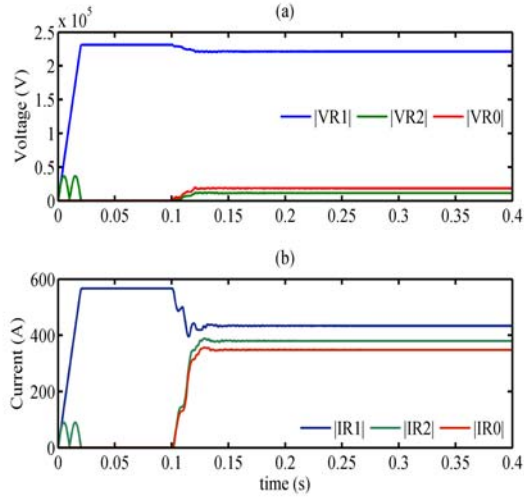


Fig. 5. Sequence voltage and current phasor amplitudes at R

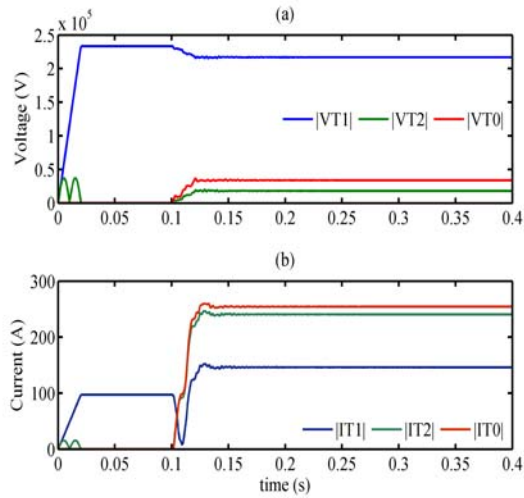


Fig. 6. Sequence voltage and current phasor amplitudes at T

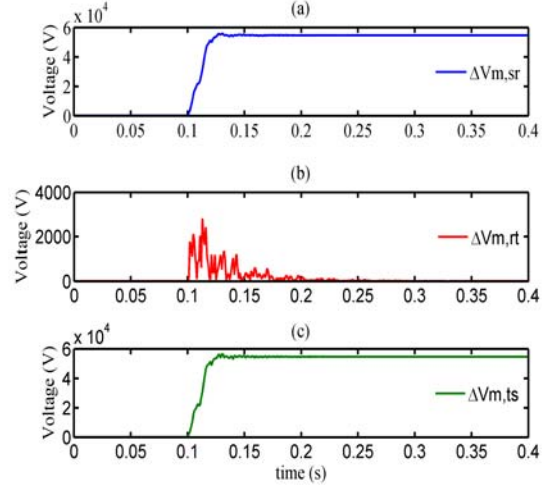


Fig. 7. Voltage differentials calculated at the tap point M of the three-terminal line

Table 1. Parameters of the power network

Components	Parameters	
	Transmission line data	r_1
x_1		0.3151 Ω/km
b_1		4.0841 $\mu\text{S}/\text{km}$
r_0		0.2750 Ω/km
x_0		1.0265 Ω/km
b_0		2.6703 $\mu\text{S}/\text{km}$
Line sections	l_1, l_2, l_3	150 km
Equivalent system at terminal S	Z_{S1}	1.312+j15.0 Ω
	Z_{S0}	2.334+j26.6 Ω
	angle of E_S	0^0
Equivalent system at terminal R	Z_{R1}	$2Z_{S1}$
	Z_{R0}	$2Z_{S0}$
	angle of E_R	30^0
Equivalent system at terminal T	Z_{T1}	$5Z_{S1}$
	Z_{T0}	$5Z_{S0}$
	angle of E_T	-10^0

Table 2. Estimated vs. actual parameters

Line parameters	Actual parameters	Estimated parameters	Error [%]
r_1 [Ω/km]	0.0276	0.0276012	0.0043
x_1 [Ω/km]	0.3151	0.3150997	0.0001
b_1 [$\mu\text{S}/\text{km}$]	4.0841	4.0840689	0.0008
r_0 [Ω/km]	0.2750	0.2766325	0.5936
x_0 [Ω/km]	1.0265	1.0277428	0.1211
b_0 [$\mu\text{S}/\text{km}$]	2.6703	2.6701166	0.0069
δ [0]	18	18.000013	0.0001
φ [0]	36	36.000007	0.0000
l [km]	60	60.010136	0.0169

The fault location estimates obtained by the proposed approach for all fault types except for single-line-to-ground faults are presented in Table 3. The fault type, fault resistance, faulted section and actual fault location are given in the 1st, 2nd, 3rd and 4th column respectively. The estimation error is displayed in the 5th column. It is evident that highly accurate results have been achieved.

Table 4 shows the results obtained for single-line-to-ground fault scenarios. Except for the fault location estimates, the zero sequence line parameter estimates are provided also. The proposed method still yields fairly accurate results.

Table 3. Fault location estimates obtained for different fault scenarios using the proposed algorithm

Fault type	Fault resistance R_f [Ω]	Faulted section	Actual fault location [km]	Fault location error [%]
A-B	1	SM	30	0.4547
		TM	120	0.0391
B-C		SM	90	0.0112
		RM	30	0.0940
C-A		TM	60	0.1322
		RM	90	0.2789
A-B-G		TM	60	0.0673
		10	SM	60
RM			30	0.1817
B-C-G	SM		90	0.1282
	RM		90	0.4989
C-A-G	TM		30	0.0697
	SM		30	0.1257
A-B-C	0	RM	120	0.0933
		TM	60	0.0080
			120	0.0203

Table 4. Fault location and zero sequence line parameter estimates obtained for single-line-to-ground faults by the proposed algorithm

Fault type	Fault resistance R_f [Ω]	Faulted section	Actual fault location [km]	Fault location error [%]	Estimated resistance r_0 error [%]	Estimated reactance x_0 error [%]	Estimated susceptance b_0 error [%]
A-G	10	SM	60	0.0169	0.5936	0.1211	0.0069
		RM	120	0.0022	0.1455	0.0292	0.0789
		TM	30	0.1360	0.2909	0.0585	0.1872
B-G		SM	60	0.0233	0.2182	0.0585	0.3063
		RM	90	0.0162	0.2545	0.1266	0.1982
		TM	120	0.0105	0.0727	0.0292	0.0863
C-G		SM	120	0.0019	0.9818	0.0682	0.0608
		RM	60	0.0055	0.0364	0.0076	0.1115
		TM	90	0.0071	0.0087	0.0098	0.1447

4 Conclusions

In this paper we have presented a novel fault location and transmission line parameter estimation algorithm for three terminal lines. The algorithm is utilizing unsynchronized fault recordings on all line terminals. The whole parts of the algorithm have been described explicitly. Evaluation studies based on ATP-EMTP simulation have demonstrated very promising results. The algorithm can yield very accurate fault location estimates, that are immune to line parameters errors, and can improve settings of distance relays and fault locators.

5 References

- [1] Koglin H.G., Schmidt M.: *Estimation of transmission line parameters by evaluating fault data records*, 12th Power System Computation Conference, 19-23.08.1996, Dresden.
- [2] Liao Y.: *Transmission line fault location algorithms without requiring line parameters*, Electric Power Components and System, vol. 36, no. 11, November 2008, pp. 1218-1225.
- [3] Liao Y., Kang N.: *Fault-location algorithms without utilizing line parameters based on the distributed parameter line model*, IEEE Transactions on Power Delivery, vol. 24, no. 2, April 2009, pp. 579-584.
- [4] Grainger J., Stevenson W.: *Power system analysis*, McGraw-Hill, New York, 1994.
- [5] Phadke A.G, Thorp J.S.: *Computer relaying for power systems*, Research Study Press, and Wiley, New York, 1988.
- [6] IEEE Standard C37.111-1991, *IEEE Standard Common Format for Transient Data Exchange (COMTRADE) for Power Systems*, Version 1.8, February 1991.
- [7] Roberts J.B., Tziouvaras D.: *Fault type selection system for identifying faults in an electric power system*, U.S. Patent 6,934,654, 2003.
- [8] Abe M., Otsuzuki N., Emura T., Takeuchi M.: *Development of a new fault location system for multi-terminal single transmission lines*, IEEE Transactions on Power Delivery, vol. 10, no. 1, January 1995, pp. 159-168.